The Canadian Mineralogist
Vol. 44, pp. 1481-1497 (2006)

CATAMARCAITE, Cu_6GeWS_8, A NEW GERMANIUM SULFIDE MINERAL SPECIES FROM CAPILLITAS, CATAMARCA, ARGENTINA: DESCRIPTION, PARAGENESIS AND CRYSTAL STRUCTURE

HUBERT PUTZ[§], WERNER H. PAAR AND DAN TOPA

Department of Material Science (*Mineralogy*), *University of Salzburg, Hellbrunnerstrasse 34, A–5020 Salzburg, Austria*

EMIL MAKOVICKY

Geological Institute, University of Copenhagen, Østervoldgade 10, DK–1350 Copenhagen, Denmark

ANDREW C. ROBERTS

Geological Survey of Canada, 601 Booth Street, Ottawa, Ontario K1A 0E8, Canada

ABSTRACT

Catamarcaite, ideally Cu_6GeWS_8, was discovered in bornite-rich ore from old dumps near the La Rosario vein, Capillitas epithermal deposit, Catamarca Province, Argentina. The new mineral is associated with bornite, digenite, chalcocite, covellite, sphalerite, hübnerite, luzonite, wittichenite, several Ge-bearing sulfides (putzite, unnamed $Cu_8Fe_2ZnGe_2S_{12}$, and a briartite-type phase) and quartz. Catamarcaite occurs as a thin rim lining cavities and fractures in chalcocite–bornite ore, and as aggregates, up to 1 mm in size, composed of anhedral to subhedral, intensely twinned grains within digenite – chalcocite – sphalerite ore. The mineral is opaque, grey, has a metallic luster and a black streak. It is brittle, and the fracture is irregular to subconchoidal. Neither cleavage nor parting is evident in polished sections. VHN_{25} ranges between 193 and 264 (mean 227) kg/mm^2, which corresponds to a Mohs hardness of 3½. The density could not be measured because of the small grain-size. Using the ideal formula and the unit-cell parameters from powder data, the calculated density is 4.892 g/cm^3. In plane-polarized reflected light, catamarcaite is greyish white with a distinct brownish tint. It shows no pleochroism, and the bireflectance is absent in air and very weak in oil. Between crossed polars, it is weakly anisotropic in shades of grey. In oil and between slightly uncrossed polars, the rotation tints are pinkish grey to bluish green. Red internal reflections are occasionally observed along fractures. The reflectance values (in air and in oil, interval 400–700 nm) are tabulated; the COM values in air are (R_1 and R_2 in %): 470 nm: 24.5, 25.2; 546 nm: 24.1, 24.5; 589 nm: 24.5, 25.1; 650 nm: 23.4, 23.7. The average result of 34 electron-microprobe analyses is: Cu 42.72, Ag 0.14, Fe 0.17, Ge 7.84, W 20.89, S 27.79, total 99.55 wt.%, corresponding to the empirical formula $Cu_{6.09}Ag_{0.01}Fe_{0.03}Ge_{0.98}W_{1.03}S_{7.86}$ (on the basis of a total of 16 atoms). The ideal formula of catamarcaite, Cu_6GeWS_8, requires Cu 42.64, Ge 8.12, W 20.56, S 28.68, total 100.00 wt.%. Catamarcaite is hexagonal, space group $P6_3mc$, with unit-cell parameter refined from single-crystal data: a 7.5238(8), c 12.390(3) Å, V = 607.4(2) Å^3, Z = 2, and c:a = 1.6467. The strongest eight X-ray powder-diffraction lines [d in Å(I)(*hkl*)] are: 5.767(100)(011), 3.215(25)(112), 3.151(35)(021), 2.884(28)(022), 2.416(26)(121), 1.972(24)(025), 1.881(48)(220) and 1.744(26)(026). The crystal structure was solved by direct methods to an R_1 index of 4.86% for 616 unique reflections measured with Mo$K\alpha$ X-radiation. Catamarcaite is a derivative of a tetrahedral *Me*S structure with a stacking, along the c axis, of the *ABAC* type, with a combined *hchc*.. sequence. Thus two-layer packets with a cubic layer stacking are invariably separated by a boundary based on the hexagonal stacking of layers of tetrahedra (*i.e.*, it is alternation of the "sphalerite" and "wurtzite" structure-types). The new mineral is chemically related to kiddcreekite, Cu_6SnWS_8, and hemusite, Cu_6SnMoS_8. The structural relationships among the three species are unknown. Catamarcaite is named after the Province of Catamarca, where the new mineral species was found. The mineral and mineral name have been approved by the Commission of New Minerals and Mineral Names, IMA (2003–020).

Keywords: catamarcaite, new mineral species, copper germanium tungsten sulfide, crystal structure, kiddcreekite, La Rosario vein, Capillitas deposit, Catamarca Province, Argentina.

SOMMAIRE

La catamarcaïte, de composition idéale Cu_6GeWS_8, a été découverte dans un minerai riche en bornite dans les haldes de la veine dite La Rosario, du gisement épithermal de Capillitas, province de Catamarca, en Argentine. Lui sont associés bornite, digé-

§ *E-mail address*: hubert.putz@sbg.ac.at

nite, chalcocite, covellite, sphalérite, hübnérite, luzonite, wittichénite, plusieurs sulfures porteurs de Ge (putzite, $Cu_8Fe_2ZnGe_2S_{12}$ sans nom, et une phase ressemblant à la briartite) et le quartz. La catamarcaïte se présente en liseré le long de cavités et de fractures dans le minerai à chalcocite–bornite, et en aggrégats atteignant 1 mm, faits de cristaux xénomorphes ou sub-idiomorphes fortement maclés au sein du minerai à digénite – chalcocite – sphalérite. Le minéral est opaque, gris, possédant un éclat métallique et une rayure noire. Il est cassant, et la fracture est irrégulière à subconchoïdale. Aucun clivage ou plan de séparation n'est évident en sections polies. Les valeurs de VHN_{25} vont de 193 à 264 (en moyenne, 227) kg/mm^2, ce qui correspond à une dureté de Mohs de 3½. On n'a pu mesurer la densité à cause de la taille des grains. En utilisant la formule idéale et les paramètres de la maille élémentaire, nous calculons une densité de 4.892 g/cm^3. En lumière polarisée réfléchie, la catamarcaïte est blanc grisâtre avec une teinte brunâtre distincte. Elle ne montre aucun pléochroïsme; il n'y a aucune biréflectance dans l'air, et elle est très faible dans l'huile. Avec nicols croisés, elle est faiblement anisotrope en teintes de gris. Dans l'huile et avec les nicols légèrement décroisés, les teintes de rotation vont du gris rosâtre à vert bleuâtre. Des réflexions internes rouges sont visibles le long de fractures. Nous présentons les valeurs de réflectance déterminées dans l'air et dans l'huile sur l'intervalle 400–700 nm; les valeurs COM dans l'air (R_1 et R_2 en %) sont: 470 nm: 24.5, 25.2; 546 nm: 24.1, 24.5; 589 nm: 24.5, 25.1; 650 nm: 23.4, 23.7. Trente-quatre analyses avec une microsonde électronique ont donné, en moyenne: Cu 42.72, Ag 0.14, Fe 0.17, Ge 7.84, W 20.89, S 27.79, pour un total de 99.55% (poids), ce qui correspond à la formule empirique $Cu_{6.09}Ag_{0.01}Fe_{0.03}Ge_{0.98}W_{1.03}S_{7.86}$ (sur une base de 16 atomes). La formule idéale de la catamarcaïte, Cu_6GeWS_8, requiert Cu 42.64, Ge 8.12, W 20.56, S 28.68, total 100.00%. La catamarcaïte est hexagonale, groupe spatial $P6_3mc$, avec les paramètres réticulaires suivants affinés à partir de données sur monocristal: a 7.5238(8), c 12.390(3) Å, V 607.4(2) Å^3, $Z = 2$, et c:a = 1.6467. Les huit raies les plus intenses du spectre de diffraction X [méthode des poudres, d en Å(I)(*hkl*)] sont: 5.767(100)(011), 3.215(25)(112), 3.151(35)(021), 2.884(28)(022), 2.416(26)(121), 1.972(24)(025), 1.881(48)(220) et 1.744(26)(026). La structure cristalline a été résolue par méthodes directes jusqu'à un résidu R_1 de 4.86% en utilisant 616 réflexions uniques mesurées avec rayonnement Mo$K\alpha$. La catamarcaïte est un dérivé de la structure à tétraèdres *Me*S avec un empilement le long de l'axe c de type *ABAC*, et donc une séquence combinée *hchc*... Une séquence de deux couches à empilement cubique est suivie d'une interface avec une maille à empilement hexagonal de tétraèdres; en autres mots, il s'agit d'une alternance de modules "sphalérite" et "wurtzite". La nouvelle espèce est chimiquement apparentée à la kiddcreekite, Cu_6SnWS_8, et la hémusite, Cu_6SnMoS_8. Les interrelations structurales parmi les trois espèces restent à définir. Le nom de l'espèce rappelle la province de Catamarca, où se trouve la localité-type. Le nom et le minéral ont reçu l'approbation de la Commission des Nouveaux Minéraux et des Noms de Minéraux (dossier 2003–020).

(Traduit par la Rédaction)

Mots-clés: catamarcaïte, nouvelle espèce minérale, sulfure de cuivre, germanium et tungstène, structure cristalline, kiddcreekite, veine La Rosario, gisement de Capillitas, province de Catamarca, Argentine.

Introduction

In the Earth's crust, germanium mainly occurs in trace amounts in silicates, though notable concentrations are known in some sulfides (*e.g.*, up to 3000 ppm in sphalerite), oxides, hydroxides and sulfates (Bernstein 1985). The enrichment of Ge in sulfide deposits, especially those containing Zn–Cu–Pb, is documented from several locations worldwide, such as Tsumeb, Namibia (Sclar & Geier 1957, Geier & Ottemann 1970a, b, 1972, Lombaard *et al.* 1986) and Kipushi, Democratic Republic of Congo (Francotte *et al.* 1965, Viaene & Moreau 1968, Intiomale & Oosterbosch 1974). Within these deposits, Ge-rich zones are usually associated with high-grade copper ore (Bernstein 1985). Germanium either occurs as an essential component of several sulfide minerals, particularly those with Cu (*e.g.*, renierite, briartite and germanite), or it substitutes for As and Sn (*e.g.*, Ge-bearing colusite). Argyrodite, ideally Ag_8GeS_6, is restricted to Ag-bearing sulfide deposits such as Freiberg, Saxony (Baumann *et al.* 1997), and Colquechaca and Porco, Bolivia (Ahlfeld & Schneider-Scherbina 1964, Paar *et al.* 2004a, Paar & Putz 2005). At Capillitas, germanium is present as a constituent of sulfides, both in high-grade copper ore (putzite, catamarcaite, unnamed $Cu_8Fe_2ZnGe_2S_{12}$ and a briartite-type phase) and in high-grade silver ore (argyrodite and "As-bearing" argyrodite) (Putz *et al.* 2002, Putz 2005, Paar & Putz 2005).

The Capillitas epithermal deposit, Department of Andalgalá, Catamarca Province, northwestern Argentina, was mined for copper, silver and gold until the beginning of the 20th century, and is presently a well-known source of gem-quality rhodochrosite. A detailed investigation of the mineralogy of the Capillitas deposit was carried out as part of a bilateral project between the Austrian (FWF) and the Argentinian (CONICET) research councils. The results are presented in Putz (2005). This study has led to the discovery of several new mineral species. Two of them, putzite (Paar *et al.* 2004b) and catamarcaite, the subject of this contribution, have already been accepted by the IMA–CNMMN (cases number 2002–024 and 2003–020, respectively).

Catamarcaite is named after the Argentinian Province of Catamarca, where the new mineral was found. Holotype material (a polished section and one fragment of ore) is deposited in the systematic collection of the Division of Mineralogy, Department of Material Science, University of Salzburg, Austria, under catalogue numbers 14931 and 14932.

Location and Geology

The Capillitas mining district (lat. 27°21'S, long. 66°23'W) is part of the Farallón Negro Volcanic Complex (FNVC), which consists of Miocene extrusive rocks, as well as intrusive subvolcanic rocks of largely andesitic composition (Fig. 1A; Sasso 1997, Sasso & Clark 1998). Intrusive rocks are restricted to various volcanic centers (Fig. 1A) and host porphyry Cu–Au deposits (*e.g.*, Bajo de la Alumbrera, Agua Rica) and epithermal vein-type deposits (Farallón Negro – Alto de la Blenda, Capillitas). The volcanic rocks overlie Tertiary continental redbeds of the El Morterito Formation. The underlying crystalline basement consists of metapelites and schists of the lower Cambrian Suncho Formation and the upper Ordovician to lower Silurian Capillitas granitic batholith (Aceñolaza *et al.* 1982).

The Capillitas diatreme, located in the granitic basement block of the Sierra de Capillitas (Figs. 1A, B), is a volcanic pipe composed of intrusive and volcanoclastic rocks of rhyolitic to dacitic composition of Miocene age (~5 Ma). The main lithologies are lapilli tuff, ignimbrite, rhyolite porphyry, lithic tuff and dacite porphyry (Breitenmoser 1999, Hug 1999). Leucocratic dikes of rhyolitic composition and melanocratic dikes of basaltic composition are exposed north and west of the diatreme. The diatreme is host to the subvolcanic, epithermal vein-type Capillitas deposit (Márquez-Zavalía 1988, 1999). This deposit has a pronounced polymetallic character and consists of numerous mineralized veins, which cross-cut the diatreme volcanic suite and the adjacent Capillitas granite north and west of the Capillitas diatreme (Fig. 1B). Two preferred orientations of the steeply dipping veins are observed: ENE–WSW (*e.g.*, La Grande, La Rosario and La Argentina veins) and WNW–ESE to NNW–SSE (*e.g.*, Capillitas, Nueve and Ortiz veins). The veins can be traced along strike from a few meters up to 800 m. Their vertical extent is unknown, but estimated to be more than 500 m. The major mineralized veins consist of numerous lenticular to tabular orebodies of variable length and width that pinch, swell and anastomose. As in other epithermal vein-type deposits, the distribution of these bonanza ores is very irregular, both along strike and dip. The thickness of the veins ranges from a few cm up to more than 2.5 m (*e.g.*, Capillitas and La Rosario veins), with an average between 50 and 70 cm (Angelelli & Rayces 1946).

Mineralization

In the Capillitas area, alteration and mineralization are restricted to the extrusive and intrusive rocks of the Capillitas diatreme and to the epithermal veins and leucocratic dikes in the vicinity of the diatreme. Alteration comprises phyllic, propylitic and argillic alteration, silicification and pyritization (Márquez-Zavalía 1999, Putz 2005). The different geological environments, the alteration features and the ore mineralogy show that high- and intermediate-sulfidation environments are present (*sensu* Sillitoe & Hedenquist 2003), and overprinted by supergene processes. The polymetallic character of the Capillitas epithermal deposit is demonstrated by its complex Cu–Pb–Zn–Fe–As–Sb paragenesis, with minor W, Bi, Sn, Te, Ag and Au, and traces of Ge, Cd, In, V, Ni and Tl (Putz 2005). On the basis of extensive exploration in the late 1970s, a total of 387,000 tonnes of ore reserves was calculated. The average grades are: Au 2.6 g/t, Ag 108 g/t, Cu 2.32%, Pb 1.62% and Zn 3.10% (Márquez-Zavalía 1999).

The high-sulfidation assemblages are typically composed of pyrite, enargite–luzonite, tennantite – tetrahedrite – goldfieldite, hübnerite, bismuth sulfosalts (*e.g.*, aikinite–bismuthinite, wittichenite), tin sulfides (*e.g.*, colusite–nekrasovite, stannoidite, mawsonite) and minor native gold, accompanied by advanced argillic alteration (quartz, dickite, svanbergite–hinsdalite) and vuggy quartz (Putz 2005). This type of mineralization represents an early stage, which is mainly restricted to the diatreme-hosted veins. It usually consists of disseminated ore that replaced or impregnated leached country-rocks; massive to banded sulfide veins are subordinate.

Intermediate-sulfidation assemblages consisting of galena, Fe-poor sphalerite, tennantite–tetrahedrite, chalcopyrite, pyrite, marcasite, rhodochrosite, quartz and barite typically occur within the granite- and rhyolite-dike-hosted veins distal with respect to the diatreme (Putz 2005). Only locally, these assemblages are enriched in sulfides and sulfosalts of Ag (acanthite, argyrodite, proustite–pyrargyrite, pearceite) and native silver (Putz 2005). Open-space filling and rhythmic banding (*e.g.*, the rhodochrosite-rich parts) are ubiquitous textural features. Vein breccias are commonly observed and usually show a cockade texture.

Ores rich in bornite – digenite – chalcocite are mainly restricted to the central part of the deposit (in the vicinity of the La Rosario vein) and show a very complex and unique mineralogy (Putz 2005). Two subtypes can be recognized. (1) Massive bornite–chalcocite ore is spatially associated with subordinate hübnerite, pyrite, chalcopyrite, tennantite, wittichenite, mawsonite and thalcusite. This type of ore contains several germanium-bearing phases: putzite, catamarcaite, unnamed $Cu_8Fe_2ZnGe_2S_{12}$, and a briartite-type phase (Paar *et al.* 2004b, Putz *et al.* 2002, Putz 2005). (2) A more stockwork-like subtype is characterized by the abundant deposition of Sn-bearing (colusite–nekrasovite, stannoidite and mawsonite) and Te-bearing minerals (*e.g.*, goldfieldite, hessite). These copper-rich ores are interpreted to be the remnants of bornite-rich, late high-sulfidation mineralization, which was overprinted by supergene mineralization, with the deposition of chalcocite, digenite, covellite and native gold (Putz 2005).

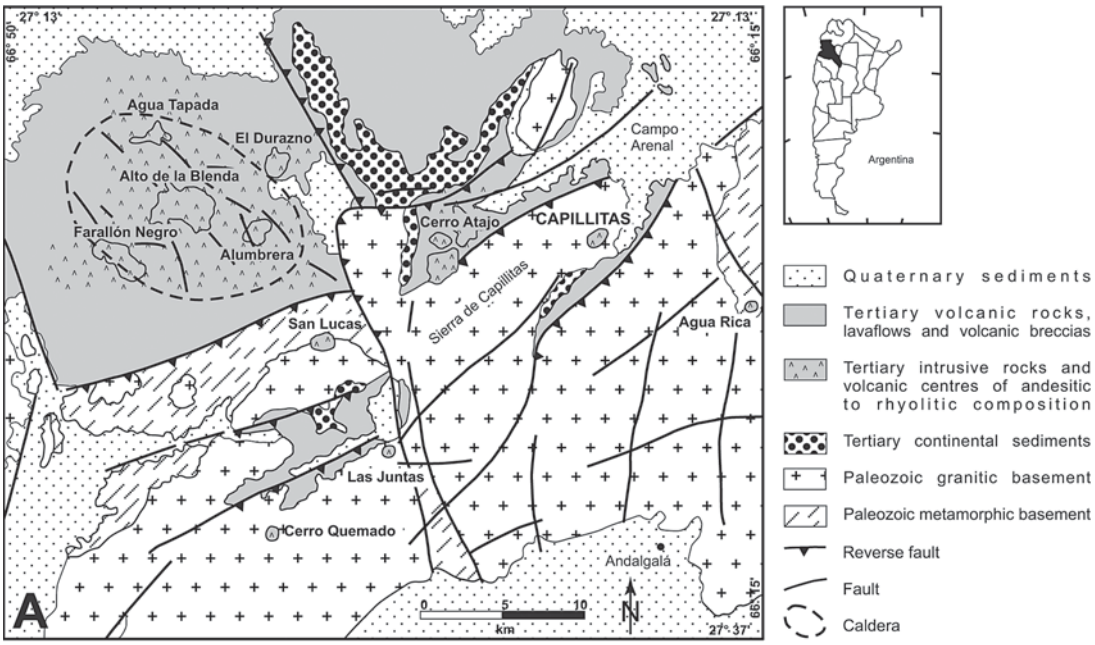
27° 13'
66° 50'
66° 15'
27° 37'
Agua Tapada
El Durazno
Alto de la Blenda
Farallón Negro
Alumbrera
Campo Arenal
Cerro Atajo
CAPILLITAS
Sierra de Capillitas
San Lucas
Agua Rica
Las Juntas
Cerro Quemado
Andalgalá
A
0 5 10
km
N
Argentina
Quaternary sediments
Tertiary volcanic rocks, lavaflows and volcanic breccias
Tertiary intrusive rocks and volcanic centres of andesitic to rhyolitic composition
Tertiary continental sediments
Paleozoic granitic basement
Paleozoic metamorphic basement
Reverse fault
Fault
Caldera

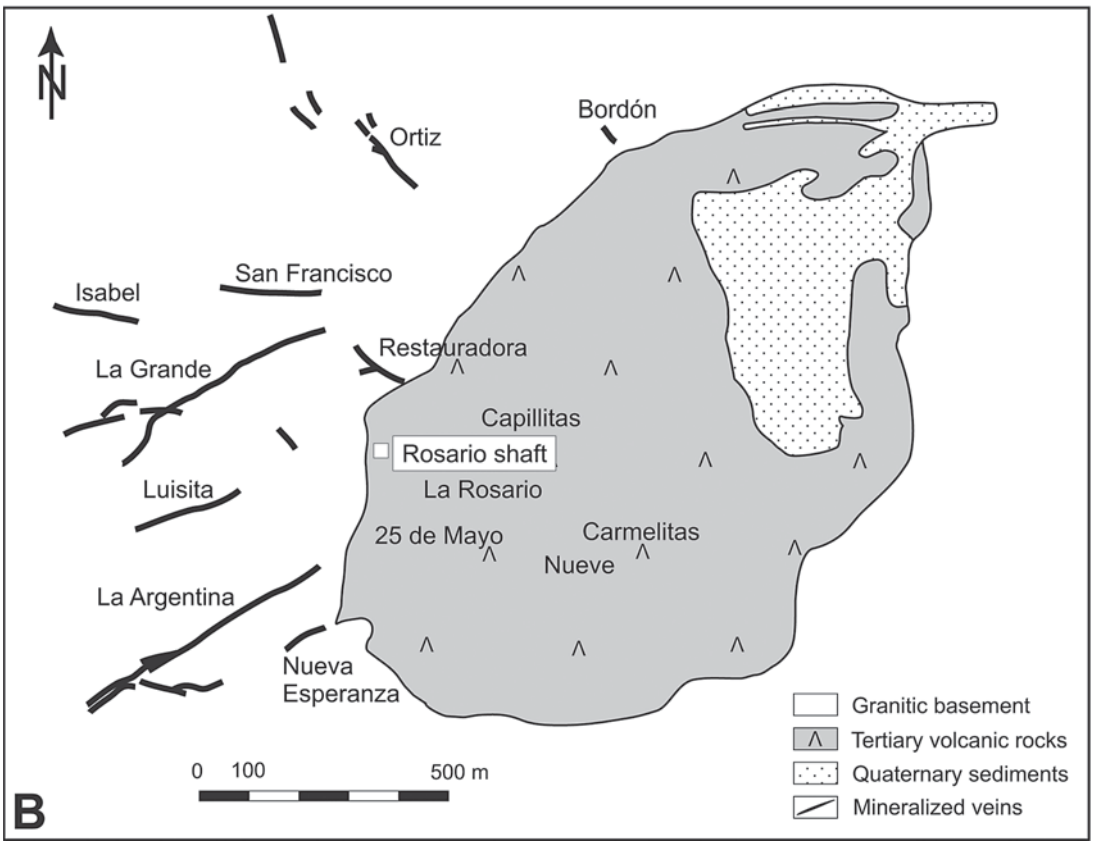
N
Ortiz
Bordón
San Francisco
Isabel
La Grande
Restauradora
Capillitas
Rosario shaft
La Rosario
Luisita
25 de Mayo
Carmelitas
Nueve
La Argentina
Nueva Esperanza
0 100 500 m
B
Granitic basement
Tertiary volcanic rocks
Quaternary sediments
Mineralized veins

An oxidation zone is developed throughout the deposit, but restricted to the uppermost 40 to 50 m of the veins. Oxides and hydroxides of Mn and Fe, cuprite, azurite, malachite, brochantite, cyanotrichite, cerussite, anglesite, beudantite and osarizawaite are common phases (Putz 2005).

Appearance and Physical Properties

The new mineral species is a rare constituent of bornite – digenite – chalcocite ore of the La Rosario vein; only two catamarcaite-bearing specimens are known. The holotype specimen, which measured 4 × 3 × 2 cm, was collected from a small pile of ore in the "Quebrada Lavadero", where high-grade copper–gold ore was concentrated. This fragment of ore was cut into several thin slices, from which four polished sections were prepared (samples X19/H8, X19/H12, X19/P and X19/P2). Within the holotype specimen, catamarcaite forms aggregates, up to 1 mm in size, composed of fractured, anhedral to subhedral grains that are arranged in a network-like texture within a quartz-bearing bornite – digenite – chalcocite – covellite – sphalerite matrix (Fig. 2a). These aggregates are usually composed of intensely twinned, lath-shaped grains (twin law unknown) showing a mosaic-like pattern (Fig. 2c); aggregates lacking twinning are rare and measure up to 55 × 120 μm. The new species is occasionally intergrown with luzonite or unnamed $Cu_8Fe_2ZnGe_2S_{12}$ (Fig. 3a), and rarely contains inclusions of wittichenite. Very rarely, the tungsten–germanium sulfide can be observed in direct contact with hübnerite (Fig. 2b).

The holotype specimen of putzite contains catamarcaite in two different habits. A thin rim (generally less than 10 μm, rarely up to 50 μm in thickness) lining cavities and fractures in bornite–chalcocite ore represents the most common type. It is composed of anhedral to euhedral grains of hexagonal shape; such rims are commonly associated with lath-shaped grains of a phase related to briartite (Fig. 3c). Less commonly, catamarcaite forms anhedral to subhedral inclusions in putzite with an envelope of unnamed $Cu_8Fe_2ZnGe_2S_{12}$ (Fig. 3b).

Catamarcaite is grey, has a metallic luster, a black streak and is opaque. The mineral is brittle and has an irregular to subconchoidal fracture. Neither cleavage nor parting is evident in polished sections. Microhardness measurements were performed with a Miniload 2 hardness tester using a load of 25 g. The Vickers hardness varies between 193 and 264 (10 indentations), mean 227 kg/mm^2. The calculated Mohs hardness is 3.5 on the basis of the equation of Young & Millman (1964). The density could not be measured because of the small grain-size. Using the unit-cell parameters derived from powder data and $Z = 2$, the calculated density based on the ideal formula is 4.892 g/cm^3, and the calculated density based on the empirical formula is 4.921 g/cm^3.

FIG. 1. a) Simplified geological map of the Farallón Negro – Capillitas area, Catamarca Province, northwestern Argentina (modified after Breitenmoser 1999). b) Simplified geological map of the Capillitas deposit (modified after Márquez-Zavalía 1988) and location of ore veins.

Optical Properties

In polished sections in plane-polarized light (~3200 K), catamarcaite is greyish white with a distinct brownish tint (Fig. 2a), which is considerably enhanced in oil. It shows no pleochroism, and the bireflectance is absent in air and very weak in oil. Between crossed polars, it is weakly anisotropic in shades of grey (Fig. 2c). In oil and between slightly uncrossed polars, its characteristic rotation-tints are pinkish grey to bluish green (quite similar to the rotation-tints of chalcocite, but somewhat less intense). Red internal reflections are occasionally observed between crossed polars, and occur along fractures and where grains are very thin (Fig. 2c). Twins are typically marked by straight lamellae of varying thickness (Fig. 2c).

Reflectance measurements were made within the visible spectrum (400–700 nm) at intervals of 20 nm using a Leitz MPV–SP microscope-spectrophotometer (Table 1, Fig. 4). A WTiC reflectance standard (Zeiss 314) was used as a reference for the air and oil (Leica N_D = 1.518) measurements. The measurements were performed on untwinned grains with a ×50 objective, the effective numerical apertures of which were confined to 0.28, and the diameters of the measured discs were 10 μm.

The shape of the reflectance spectra for catamarcaite and kiddcreekite (Bisbee, Arizona; Criddle & Stanley 1993) is very similar (Fig. 4). Catamarcaite is slightly more strongly reflecting (1–2%) than kiddcreekite (Fig. 4).

TABLE 1. REFLECTANCE DATA FOR CATAMARCAITE

λ	R_1	R_2	$^{corr}R_1$	$^{corr}R_2$	λ	R_1	R_2	$^{corr}R_1$	$^{corr}R_2$
400	24.3	25.0	10.4	10.9	560	24.4	24.8	10.3	10.6
420	24.5	25.3	10.4	10.8	580	24.5	25.1	10.5	10.9
440	24.6	25.3	10.6	11.1	589	24.5	25.1	10.5	10.8
460	24.5	25.2	10.6	11.1	600	24.5	25.0	10.4	10.8
470	24.5	25.2	10.5	11.1	620	24.0	24.5	10.3	10.5
480	24.4	25.1	10.4	10.9	640	23.6	23.9	9.8	10.0
500	24.2	24.7	10.2	10.5	650	23.4	23.7	9.7	9.8
520	24.1	24.5	10.1	10.3	660	23.1	23.3	9.5	9.7
540	24.1	24.5	10.2	10.3	680	22.6	22.8	9.1	9.2
546	24.1	24.5	10.2	10.4	700	22.2	22.4	9.0	9.0

Units: λ in nm, R in %.

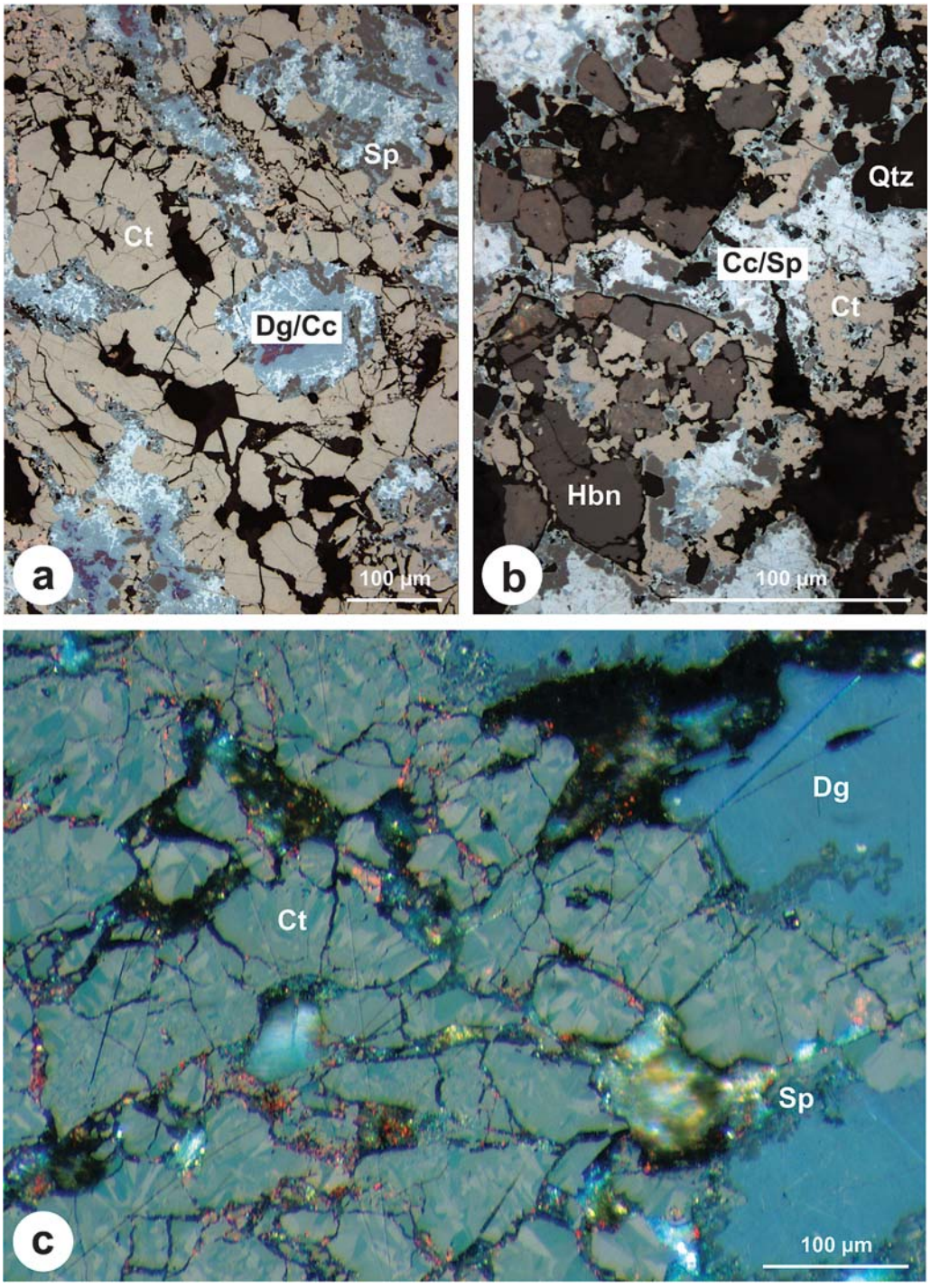

FIG. 2. a) Network-like aggregate of catamarcaite (Ct) within a bornite – digenite – chalcocite matrix (Dg/Cc) showing abundant sphalerite (Sp) (sample X19/P). b) Hübnerite (Hbn) was replaced by catamarcaite (Ct), which itself was replaced by chalcocite – sphalerite (Cc/Sp); Qtz is quartz (sample X19/H12). c) Fractured aggregate of catamarcaite (Ct) composed of twinned grains with red internal reflections; Dg is digenite, Sp sphalerite. Oil immersion, crossed polars (sample X19/P2).

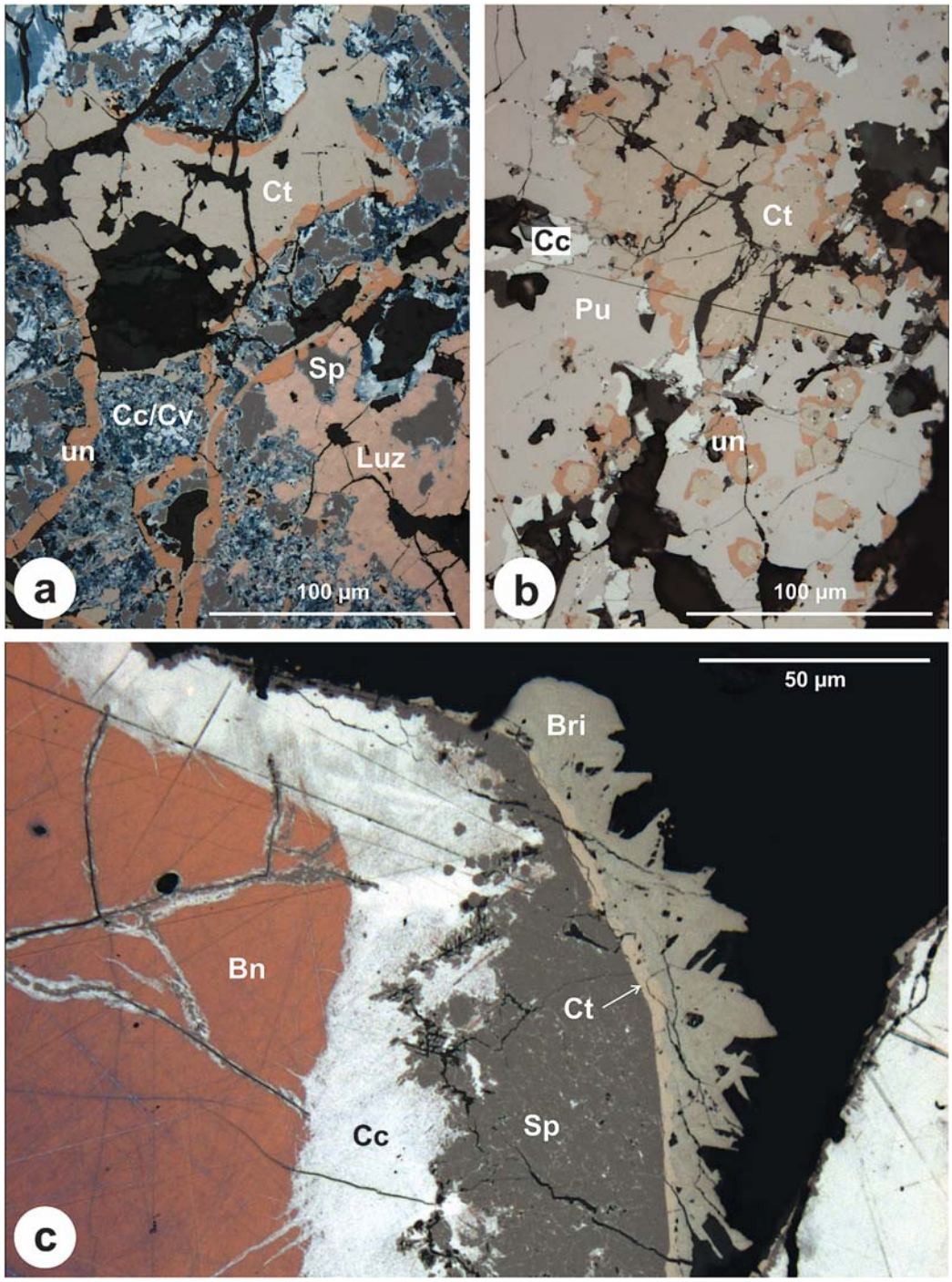

FIG. 3. a) Catamarcaite (Ct) in contact with luzonite (Luz), unnamed $Cu_8Fe_2ZnGe_2S_{12}$ (un), sphalerite (Sp) and fine-grained chalcocite – covellite (Cc/Cv) (sample X19/H12). b) Anhedral inclusions of catamarcaite (Ct) in putzite (Pu) with an envelope of unnamed $Cu_8Fe_2ZnGe_2S_{12}$ (un); putzite is replaced by chalcocite (Cc) (sample PR/C3P). c) Briartite-type phase (Bri) in close association with catamarcaite (Ct) lining a cavity in massive bornite (Bn) – chalcocite (Cc) ore; Sp is sphalerite (sample PR/C2).

Chemical Composition

Quantitative chemical data for catamarcaite and the associated germanium phases were obtained with an electron microprobe (JEOL Superprobe JXA–8600, controlled by an LINK–*eXL* system, operated at 25 kV and 35 nA), installed at the University of Salzburg. The following standards and X-ray lines were used: natural $CuFeS_2$ (chalcopyrite; Cu*K*α, Fe*K*α), synthetic ZnS (sphalerite; Zn*K*α, S*K*α), InAs (In*L*α), Ge metal (Ge*K*α), Ag (Ag*L*α) metal and W metal (W*L*α). Both Cd and Sn were sought, but not detected. The raw data were corrected with the on-line ZAF–4 procedure. The standard deviations (error in wt.%) for the major elements constituting catamarcaite are: W 0.11, S 0.08, Cu 0.07 and Ge 0.04.

The results, obtained from eight aggregates in two polished sections of the holotype specimen, show only minor variation of the chemical composition (Table 2). The average result of 34 point-analyses of four grain aggregates in sample 1 (polished section X19/P) is: Cu 42.72, Ag 0.14, Fe 0.17, Ge 7.84, W 20.89, S 27.79, total 99.55 wt.%, corresponding to $Cu_{6.09}Ag_{0.01}Fe_{0.03}Ge_{0.98}W_{1.03}S_{7.86}$ (on the basis of a total of 16 atoms). Sample 2 (polished section X19/H8) yielded the empirical formula $Cu_{6.08}Ag_{0.01}Fe_{0.06}Ge_{0.97}W_{1.01}S_{7.87}$ (average result of 19 point-analyses). Most analyses reveal traces of silver (up to 0.25 wt.% Ag) and minor amounts of iron (usually below 0.3 wt.%, rarely up to 0.6 wt.% Fe). On the basis of *Me*:S = 1:1 and *Me* + S = 16, the ideal formula of catamarcaite is Cu_6GeWS_8 and requires Cu 42.64, Ge 8.12, W 20.56, S 28.68, total 100.00 wt.%. On the basis of the crystal-structure refinement, the valences can be written as $Cu^{+}{}_6Ge^{4+}W^{6+}S^{2-}{}_8$. Several grains of catamarcaite in sample 1 (polished section X19/P) show a significant enrichment in iron and give the composition $Cu_{6.04}Ag_{0.01}Fe_{0.16}Ge_{0.98}W_{0.95}S_{7.86}$ (average result of 10 point-analyses; Table 2). Iron substituting for tungsten, with $2Fe^{3+} \rightleftharpoons W^{6+}$, is a possible mechanism.

The chemical composition of the associated putzite, ideally $(Cu_{4.7}Ag_{3.3})_{\Sigma 8}GeS_6$, is presented in detail in Paar *et al.* (2004b). Table 3 shows the composition of the two other associated germanium-bearing phases. Phase #1 (unnamed $Cu_8Fe_2ZnGe_2S_{12}$) is characterized by a composition within the range $Cu_{7.90–8.18}Fe_{1.94–2.20}Zn_{0.80–1.10}In_{0.00–0.03}Ge_{1.83–1.99}S_{11.90–12.09}$ (n = 45; Table 3). Using the ideal formula of stannoidite, $Cu_8(Fe,Zn)_3Sn_2S_{12}$ and Σ*Me* + S = 25, the empirical formula is $Cu_{8.04}(Fe_{2.03}In_{0.02})_{\Sigma 2.05}Zn_{0.96}Ge_{1.94}S_{12.01}$. In accordance with Yamanaka & Kato (1976), the ideal formula of phase #1 can be expressed as $Cu^{+}{}_8Zn^{2+}Fe^{3+}{}_2Ge^{4+}{}_2S_{12}$; thus it possibly represents the germanium analogue of stannoidite. Phase #2 (the briartite-type phase) has the average composition (n = 12) Cu 34.29, Zn 14.59, Fe 0.57, Ge 17.28, S 33.19, total 99.92 wt.% (Table 3). Using the ideal formula $Cu_2(Zn,Fe)GeS_4$ and Σ*Me* + S = 8, the empirical formula can be written as $Cu_{2.11}(Zn_{0.87}Fe_{0.04})_{\Sigma 0.91}Ge_{0.93}S_{4.05}$. Chemically, this phase corresponds to briartite.

X-Ray Crystallography

X-ray powder diffraction

Single-crystal precession studies of two anhedral fragments extracted from a polished section (X19/H8) of the holotype specimen, employing Zr-filtered Mo radiation, show that catamarcaite is hexagonal, with unit-cell parameters a 7.58 and c 12.51 Å. One fragment was mounted in such a way that 100* is parallel to the dial axis, and the other fragment was mounted such that c* is parallel to the dial axis. The following levels were photographed: $hk0 \rightarrow hk2$, $h0l$, $h1l$ and 110* ∧ a*. The diffraction symmetry observed on both zero- and upper-level *hkn* films is 6/*mmm*, and the only systematic

TABLE 2. COMPOSITION OF CATAMARCAITE FROM CAPILLITAS, ARGENTINA

Sample			Cu	Ag	Fe	Ge	W	S	Total
X19/P	n = 34	mean	42.72	0.14	0.17	7.84	20.89	27.79	99.55
		s.d.[1]	0.15	0.07	0.06	0.09	0.26	0.13	0.39
		min	42.46	0.00	0.08	7.54	20.20	27.50	98.83
		max	42.96	0.25	0.29	8.05	21.48	28.05	100.31
X19/H8	n = 19	mean	42.75	0.09	0.39	7.75	20.62	27.92	99.52
		s.d.[1]	0.19	0.06	0.11	0.11	0.23	0.15	0.39
		min	42.51	0.00	0.17	7.56	20.27	27.73	98.91
		max	43.14	0.21	0.58	7.92	21.00	28.24	100.21
X19/P	n = 10	mean	42.85	0.07	1.00	7.90	19.49	28.13	99.44
		s.d.	0.20	0.04	0.06	0.04	0.17	0.11	0.30
		min	42.57	0.00	0.89	7.84	19.18	27.96	99.03
		max	43.14	0.13	1.08	7.95	19.72	28.30	99.86
		formula (Σ*Me* + S = 16)							
X19/P	Fe-poor		6.09	0.01	0.03	0.98	1.03	7.86	
X19/H8			6.08	0.01	0.06	0.97	1.01	7.87	
X19/P	Fe-rich		6.04	0.01	0.16	0.98	0.95	7.86	

[1] standard deviation.

TABLE 3. COMPOSITION OF UNNAMED $Cu_8Fe_2ZnGe_2S_{12}$ AND OF A BRIARTITE-TYPE PHASE FROM CAPILLITAS, ARGENTINA

No.	Mineral		Cu	Fe	Zn	In	Ge	S	Total
1	unnamed	mean	42.18	9.37	5.17	0.20	11.62	31.80	100.34
	$Cu_8Fe_2ZnGe_2S_{12}$	s.d.[1]	0.34	0.26	0.43	0.06	0.22	0.20	0.46
	(n = 45)	min	41.46	8.94	4.30	0.10	11.04	31.41	99.33
		max	43.13	10.20	5.96	0.30	12.02	32.30	101.13
2	briartite-type	mean	34.29	0.57	14.59	0.00	17.28	33.19	99.92
	phase	s.d.	0.38	0.23	0.44	0.00	0.26	0.21	0.38
	(n = 12)	min	33.78	0.29	13.46	0.00	16.83	32.96	99.35
		max	35.13	1.10	15.19	0.00	17.55	33.69	100.58

[1] standard deviation. Empirical formulae: 1) $Cu_{8.04}(Fe_{2.03}In_{0.02})_{\Sigma 2.05}Zn_{0.96}Ge_{1.94}S_{12.01}$; 2) $Cu_{2.11}(Zn_{0.87}Fe_{0.04})_{\Sigma 0.91}Ge_{0.93}S_{4.05}$.

absence is *hhl* with $l = 2n$; the permissible choices of space-group are $P6_3/mmc$ (194), $P\bar{6}2c$ (190) or $P6_3mc$ (186) (diffraction aspect $P6/{**}c$). Neither of these two fragments was suitable for a crystal-structure determination. The refined unit-cell parameters, *a* 7.523(3), *c* 12.384(3) Å, *V* 606.9(4) Å^3, *c*/*a* 1.6462, are based on 19 X-ray powder lines between 3.493 and 1.608 Å for which unambiguous indexing, based on visual inspection of single-crystal precession films, was possible. The X-ray powder-diffraction experimental data, as well as two theoretical powder patterns (one calculated from powder and the second calculated from the crystal-structure refinement) are presented in Table 4.

Single-crystal X-ray diffraction

For the single-crystal investigation, several fragments of catamarcaite, mechanically extracted from a polished section (X19/P) of the holotype specimen, were investigated with a Bruker AXS diffractometer equipped with a CCD area detector using graphite-monochromatized Mo*K*α radiation. After many trials, an irregular and untwinned fragment measuring approximately 60 × 40 × 30 μm was found to be suitable for the structural investigation. Experimental settings for the catamarcaite material studied are listed in Table 5. The SMART (Bruker AXS 1998a) system of programs was used for unit-cell determination and data collection, SAINT+ (Bruker AXS 1998b) for the calculation of integrated intensities, and XPREP (Bruker AXS 1998c) for empirical absorption-correction based on pseudo Ψ-scans. The non-centrosymmetric space-group $P6_3mc$, proposed by the XPREP program, was chosen, and it is consistent with the hexagonal symmetry of the lattice and intensity statistics (mean $|E^2 - 1| = 0.799$). The structure of catamarcaite was solved by direct methods (program SHELXS of Sheldrick 1997a) that revealed most of the atom positions. In subsequent cycles of the refinement (program SHELXL of Sheldrick 1997b), the positions of additional atoms were deduced from difference-Fourier syntheses by selecting from among the strongest maxima at appropriate distances. Refinement results are given in Table 6, and fractional atomic coordinates and isotropic and anisotropic displacement parameters are listed in Table 7. Selected *Me*–S bond distances are presented in Table 8, and selected geometrical parameters for individual coordination polyhedra, calculated with IVTON program (Balić-Žunić & Vicković 1996), are given in Table 9. The table of structure factors for catamarcaite may be obtained from the Depository of Unpublished Data, CISTI, National Research Council, Ottawa, Ontario K1A 0S2, Canada.

THE CRYSTAL STRUCTURE OF CATAMARCAITE

The crystal structure of catamarcaite (Figs. 5–9) contains four different types of coordination tetrahedra: two distinct copper sites, a germanium site and a tungsten site. There are four distinct sulfur sites in the

TABLE 4. X-RAY POWDER-DIFFRACTION DATA FOR CATAMARCAITE

	I_{est}	$I^{\#}_{calc}$	d_{meas}	d_{calc}	$d^{\#}_{calc}$	*hkl*		I_{est}	$I^{\#}_{calc}$	d_{meas}	d_{calc}	$d^{\#}_{calc}$	*hkl*
		2			6.516	010	*	25	16	2.243	2.244	2.2449	024
	40	19	6.183	6.192	6.195	002		3	2	2.173	2.172	2.1719	030
	100	100	5.782	5.766	5.767	011	*	10	4	2.113	2.115	2.1152	123
	20	14	4.484	4.488	4.490	012		10	2	2.052	2.064	2.0650	006
	10	7	3.786	3.762	3.762	110			7		2.049	2.0496	032
*	20	13	3.493	3.487	3.488	013	*	50	24	1.971	1.972	1.9723	025
*	5	8	3.267	3.258	3.258	020	*	5	3	1.927	1.927	1.9277	124
*	30	25	3.215	3.215	3.215	112	*	60	48	1.881	1.881	1.8810	220
*	40	35	3.153	3.150	3.151	021	*	5	6	1.810	1.810	1.8102	116
*	30	16	3.095	3.096	3.098	004			4			1.7998	222
*	40	28	2.887	2.883	2.8835	022		10	8	1.782	1.788	1.7882	131
*	5	7	2.799	2.796	2.7975	014			6		1.778	1.7783	034
*	15	12	2.553	2.557	2.5579	023			2			1.7468	125
	3	2	2.458	2.463	2.4627	120	*	50	26	1.744	1.744	1.7442	026
*	40	26	2.417	2.415	2.4155	121			2			1.7349	132
*	20	15	2.395	2.390	2.3912	114	*	5	4	1.707	1.707	1.7081	017
	3	4	2.318	2.315	2.3162	015	*	5	3	1.655	1.655	1.6556	133
	3	4	2.286	2.288	2.2885	122		4				1.6151	041
							*	20	9	1.608	1.607	1.6077	224

114.6 mm Debye–Scherrer powder camera; Cu radiation, Ni-filter (λ Cu*K*α = 1.54178 Å). Intensities visually estimated. Not corrected for shrinkage, and no internal standard. An asterisk (*) indicates the lines used for unit-cell refinement. Weak reflections ascribable to admixed digenite have been deleted from the powder data. Indexed on *a* 7.523, *c* 12.384 Å. #: calculated from single-crystal data using PowderCell 2.3 software (Kraus & Nolze 1999) for Debye–Scherrer geometry and Cu*K*α radiation (λ = 1.540598 Å), without the anomalous dispersion correction.

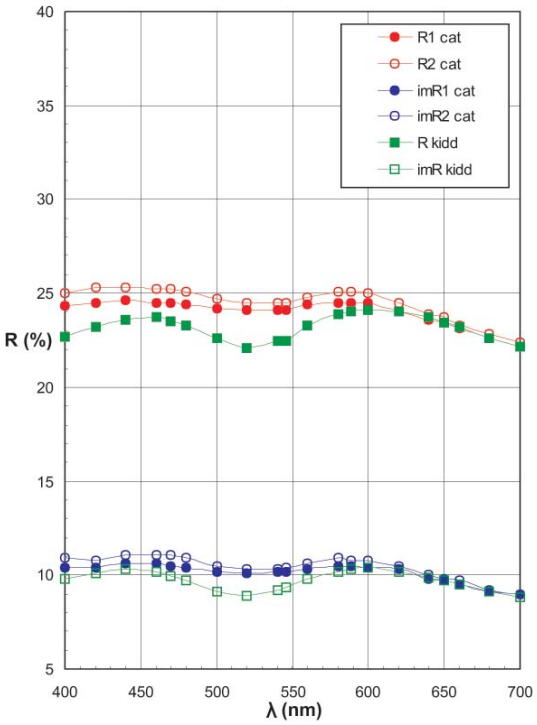

FIG. 4. Reflectance spectra, in air and in immersion oil, for catamarcaite (R_1 cat, R_2 cat, $^{im}R_1$ cat, $^{im}R_2$ cat) and kiddcreekite (R kidd, ^{im}R kidd).

structure. The germanium and tungsten sites, as well as the two sulfur sites forming a part of their polyhedra, have special values of x and y, whereas the rest are in general positions. Catamarcaite is a derivative of a tetrahedral *Me*S structure with a stacking, along the c axis, of the *ABAC* type, with a combined *hchc*.. sequence (Fig. 5). Thus, two-layer packets with a cubic layer-stacking are invariably separated by a boundary based on the hexagonal stacking of layers of tetrahedra (*i.e.*, it is alternation of the "sphalerite" and "wurtzite" principle). The alternative, "wurtzite-based" packets with a hexagonal stacking principle combine layers of tetrahedra from two adjacent cubic packets. In the direction of tetrahedron apices, the top layer of the "sphalerite-like" packet is composed of Cu1 tetrahedra with one-quarter of the tetrahedra in the layer empty. The Cu1 tetrahedra are disposed as asymmetric rows along the <100> directions of the catamarcaite lattice. In the second bottom layer, the Cu, Ge and W tetrahedra combine.

Germanium tetrahedra are positioned below the points of intersection of the <100> rows of Cu1 tetrahedra in the top layer, *i.e.*, they lie at (0, 0, z) and the equivalent positions. In the <100> directions, they are interspaced by Cu2 tetrahedra. Thus, in the configuration of the second layer, they assume positions analogous to the vacancies in the first layer, although these vacancies are situated at a different site, at ($^1/_3$, $^2/_3$, z) of the cell.

The tungsten tetrahedra share edges with three Cu2 tetrahedra in the same layer, organized around a common vertex, and with three Cu1 tetrahedra of the layer of tetrahedra above them, in the same cubic packet. Every Cu1 and Cu2 tetrahedron shares an edge

TABLE 5. SINGLE-CRYSTAL X-RAY DIFFRACTION: EXPERIMENTAL DETAILS

Diffractometer	Bruker AXS CCD system
X-ray radiation source	fine-focus sealed tube, Mo$K\alpha$
X-ray radiation monochromator	graphite
X-ray power	50 kV, 30 mA
Temperature	298 K
Rotation width	0.3°
Frame size (in pixels)	512 * 512 pixels
Resolution (Å)	0.75
Crystal form	irregular
Crystal color	metallic
Cell setting	hexagonal
Space group	$P6_3mc$
Z	2
Absorption method	empirical
Refinement	on F_o^2
Source of scattering factors	*International Tables for X-Ray Crystallography* (1992, Vol. C, Tables 4.2.6.8 and 6.1.1.4)
Structure solution	SHELXS-97 (Sheldrick 1997a)
Structure refinement	SHELXL-97 (Sheldrick 1997b)

$R_{INT} = \Sigma |F_o^2 - F_o^2(\text{mean})| / \Sigma F_o^2$
$R_1 = \Sigma ||F_o| - |F_c|| / \Sigma |F_o|$
Goof = $\{(\Sigma w[F_o^2 - F_c^2] / [n - p])\}^{½}$
$P = [\max(F_o^2, 0) + 2 F_c^2] / 3$
$R_\sigma = \Sigma \sigma(F_o^2) / \Sigma F_o^2$
$wR_2 = \{(\Sigma w[F_o^2 - F_c^2]^2 / \Sigma w[F_o^2]^2)\}^{½}$
$w = 1 / (\sigma^2[F_o^2] + [0.2 * P]^2)$

TABLE 6. SINGLE-CRYSTAL X-RAY-DIFFRACTION REFINEMENT OF THE STRUCTURE: DETAILS

Formula	Cu_6GeWS_8
Formula weight	894.16
a (Å)	7.5238(8)
b (Å)	7.5238(8)
c (Å)	12.390(3)
V (Å^3)	607.4(2)
D_x (Mg m^{-3})	4.89
Crystal size (mm)	0.06 × 0.04 × 0.03
μ (mm^{-1})	23.48
Time per frame (s)	15
Total number of frames	3599
T_{min}, T_{max}	0.465, 0.622
Maximum 2θ (°)	56.64
Measured reflections	9154
Index range	$-9 \le h \le 9$, $-9 \le k \le 9$, $-16 \le l \le 16$
Unique reflections	616
Reflections > 2σ(I)	556
R_{INT} (%)	12.24
R_σ (%)	4.39
Number of least-sqares parameters	42
GooF	0.928
R_1, $F_o > 4\ \sigma(F_o)$ (%)	4.86
R_1, all data (%)	5.44
wR_2 (on F_o^2) (%)	11.27
Final difference-Fourier map (Å^{-3})	−1.288 to + 2.751

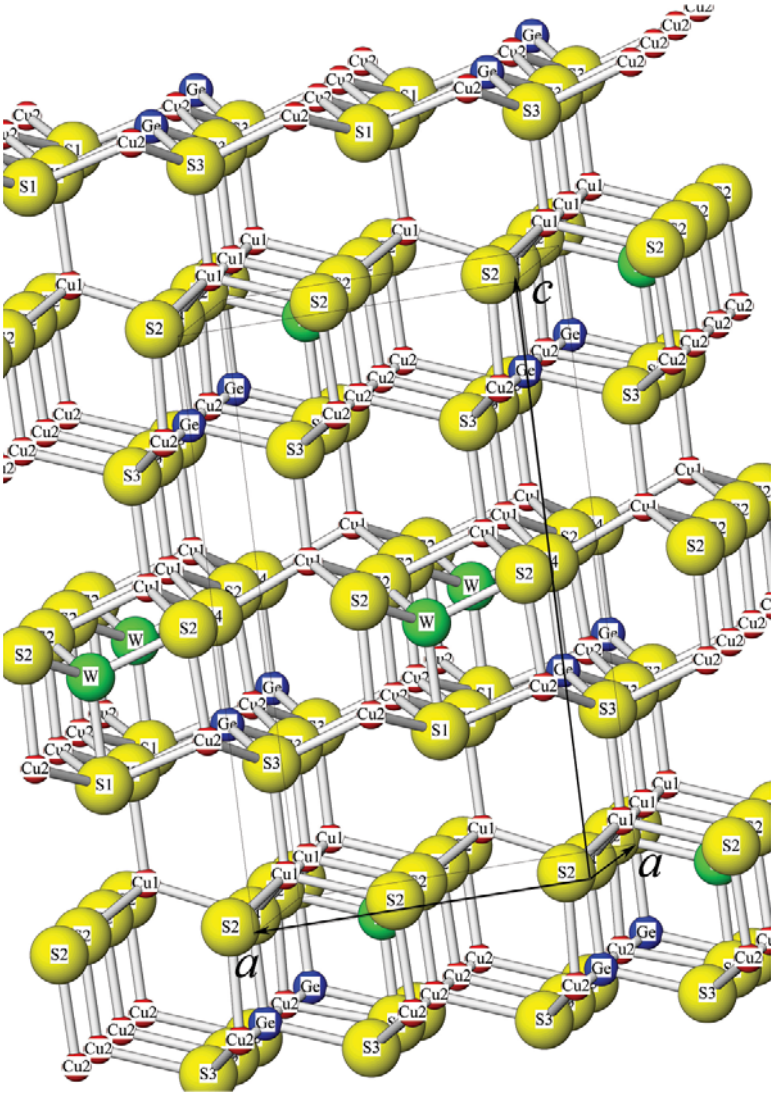

FIG. 5. The crystal structure of catamarcaite Cu_6GeWS_8. Note the *hchc*.... sequence of layers (0001) of coordination tetrahedra of Cu and Ge, as well as the W tetrahedra that are interstitial to those in the layers.

with the W tetrahedron. In contrast, the Ge tetrahedra only share vertices with the four surrounding Cu tetrahedra. There are two Ge-containing layers in a unit cell. The Ge tetrahedra in both of them are on the (0, 0, z) rows; they are $z = ½$ apart and in opposing orientation. Similarly, the W-based cluster of edge-sharing tetrahedra at ($^1/_3$, $^2/_3$, z) is followed by a 180°-rotated one at ($^2/_3$, $^1/_3$, $z + ½$).

Coordination polyhedra

Primarily because of the close association with the highly charged and small W^{6+} cation, the tetrahedra of Cu1 and Cu2 are slightly irregular, with three or four somewhat different Cu–S distances. For both of them, the Cu–S distances to the S atoms shared with the W tetrahedron are the longest ones, and the S–Cu–S

angle subtended by them is close to 104°, whereas the opposing one is ~114°. The remaining angles lie within the range 108.5–110.9°. The Cu2 tetrahedron is marginally larger than the Cu1 tetrahedron (the average bond-length is 2.310 Å for Cu1 *versus* 2.322 Å for Cu2). The atom Cu2 must form a layer that matches the Cu1 layer; thus Cu2 is combined with the smaller polyhedra of germanium (average bond-length is 2.237 Å) and W (average bond-length is 2.255 Å). In connection with the insertion of smaller, "upside-down" tetrahedra of W, the S1–S3 net at the base of the Cu2 tetrahedra is slightly warped, and S1, which is the apex of the W tetrahedron, is drawn toward W, resulting in its slightly higher *z* value (Table 7). Similarly, S4 is a bit below S2, being the apical S atom of the smaller Ge tetrahedron below it. The 6+ valence of W appears corroborated by the interatomic distance, W–S = 2.255 Å, in agreement with Shannon's (1976) tabulated ionic radii: r (radius) W^{6+} = 0.42 Å, compared to r 0.635 Å for Cu^{+} and r 0.39 Å for Ge^{4+}.

The cluster of three Cu1 and three Cu2 tetrahedra that share edges with the central "upside-down" W tetrahedron appears as a large "super-tetrahedron", with three Cu tetrahedra forming each face, and the Ge tetrahedra in three corners, whereas the fourth corner, along the [001] direction, is cut off by the occurrence of hexagonal stacking. These incomplete "supertetrahedra" alternate with tetrahedral cavities based on a missing tetrahedron in the Cu1 layers.

The "supercavities" have the groups of three tetrahedra from four adjacent W-based "supertetrahedra" (clusters) as the walls, but their [001] vertex is truncated. The valence of S atoms in the center of the walls (triplets of Cu tetrahedra) is satisfied by bonds to three atoms of Cu and one atom of W; the trigonal pyramidal coordination suggests a possibility that lone-electron pairs of these S1 and S2 point into the cavity.

Bond-valence calculations (Table 9) confirm the valence of W (5.76+), Ge (3.82+), Cu1 and Cu2 (1.19+ and 1.15+, respectively) as well as of S1 (2.35–), S2 (2.26–), S3 (1.84–) and S4 (1.96–). The formation of the "supertetrahedra" is a consequence of the strong drive of W to form short *Me–Me* interactions. In the current case, the metals Cu and W form a regular octahedron with Cu–W bond lengths equal to 2.73 Å.

Hemusite and kiddcreekite

Hemusite, ideally Cu_6SnMoS_8 (Terziev 1971, Shimizu *et al*. 1991) and kiddcreekite, ideally Cu_6SnWS_8 (Harris *et al*. 1984) are cubic minerals with *a* equal to 10.821 Å and 10.856 Å, respectively. X-ray powder data on these minerals were obtained from small amounts of polycrystalline, multicomponent, impure material. Terziev (1971) did not give further details about the purity of his specimen, and his indexing does not seem to suggest any centering of the unit cell. Harris *et al*. (1984) clearly indicated diffraction symmetry *F**** for their material. Therefore, pending further clarification of the hemusite question, the ensuing derivations apply to kiddcreekite.

The cubic, *F*-centered structure of kiddcreekite (Fig. 10) can be derived by stacking of double layers of the type defined in the previous section according to the cubic (sphalerite) and not the hexagonal (wurtzite) principle. These double layers display a cubic stacking of component layers inside them and the Cu2–Sn–W tier overlain by the Cu1 – vacancy tier. Because of the cubic stacking, the W-based cluster of the double layer #2 will be superimposed over the vacancy in the double layer #1; the Ge tetrahedron of the second double layer will be placed over the W-based cluster of the initial double layer (it will be attached to the "outer" sulfur atoms of its Cu1 component) and the cavity will come over the Cu1 tetrahedra situated above the Ge tetrahedron of the double layer #1. Repeating this process, the fourth double layer gives a complete *F*-centered cubic cell, with [111] being the *ABC* stacking sequence of double layers.

The cubic stacking changes the truncated W-based cluster into a complete "supertetrahedron" with four Ge vertices. Adjacent "supertetrahedra" overlap by sharing these Ge configurations, as they also do in catamarcaite, but there only in the (0001) planes. Thus, the structure

TABLE 7. ATOM PARAMETERS FOR CATAMARCAITE

Atom	*x/a*	*y/b*	*z/c*	U_{11}	U_{22}	U_{33}	U_{23}	U_{13}	U_{12}	U_{eq}
W	0.33333	0.66667	0.4810(2)	0.0103(3)	0.0103(3)	0.0051(4)	0	0	0.0051(2)	0.0085(3)
Cu1	0.8402(2)	0.1598(2)	0.1049(2)	0.022(1)	0.022(1)	0.013(1)	0.0016(5)	-0.0016(5)	0.0137(9)	0.0177(6)
Cu2	0.5044(2)	0.4956(2)	0.3536(2)	0.0197(9)	0.0197(9)	0.0166(9)	-0.0015(5)	0.0015(5)	0.0094(9)	0.0189(6)
Ge	0	0	0.3513(2)	0.0100(9)	0.0100(9)	0.006(1)	0	0	0.0050(4)	0.0085(6)
S1	0.33333	0.66667	0.3002(6)	0.020(3)	0.020(3)	0.009(3)	0	0	0.010(1)	0.016(2)
S2	0.5032(3)	0.4969(3)	0.0419(4)	0.016(2)	0.016(2)	0.009(3)	0.0016(9)	-0.0016(9)	0.006(2)	0.0142(1)
S3	0.8381(3)	0.6763(6)	0.29044)	0.012(2)	0.010(2)	0.010(2)	-0.001(2)	-0.0002(8)	0.005(1)	0.011(1)
S4	0	0	0.5311(7)	0.015(2)	0.015(2)	0.004(3)	0	0	0.007(1)	0.011(1)

of kiddcreekite is a three-dimensional stacking of W-based "supertetrahedra" with common Ge vertices. This model also offers a simple explanation of the intimate twinning of catamarcaite, difficult to explain from the structure itself. A cubic nucleus or a defect, with Ge atoms assuming all four corners of a supertetrahedron, can lead to four orientations of the catamarcaite structure, with (0001) parallel to four {111} planes of the cubic *intermezzo*.

The different crystallography of catamarcaite and kiddcreekite is apparently due to the difference in the Me^{4+} tetrahedra: the radius of $^{IV}Ge^{4+}$ is 0.39 Å, whereas that of $^{IV}Sn^{4+}$ is larger (0.55 Å: Shannon 1976), implying a lesser amount of ditrigonalization of the Cu2 framework than observed in catamarcaite.

Relationship To Other Minerals

Catamarcaite is clearly distinct from all the other natural germanium–tungsten-bearing compounds, which belong to the colusite group of sulfides. Colusite from polymetallic ore deposits usually contains significant amounts of germanium or tungsten. Up to 5 wt.% Ge was detected in colusite from the Waterloo deposit, Australia (Wagner & Monecke 2005), and approximately 2 wt.% W occurs in colusite–nekrasovite from Bisbee, Arizona, USA (unpubl. data, H. Putz). "Vanadium-germanite", a V-bearing variety of germanite from Tsumeb, Namibia, was reported by Geier & Ottemann (1970a). This phase was later established by Spiridonov *et al*. (1992) as germanocolusite, ideally $Cu_{26}V_2(Ge,As)_6S_{32}$, and thus the Ge-analogue of colusite. The first evidence of tungsten as an essential element in germanite was also recorded in material from Tsumeb, for which the name "tungsten-germanite" had been suggested (Geier & Ottemann 1970b). However, this phase caused some confusion in the literature, and its full characterization as a valid species needed several decades. In 1992, it was approved by the IMA–CNMMN (IMA 1992–039) and subsequently published as unnamed $Cu_{20}(Fe,Cu,Zn)_6W_2Ge_6S_{32}$ (Spiridonov 1994). A full description of this phase, under the name of ovamboite (IMA 1992–039 = "tungsten-germanite"), was published recently (Spiridonov 2003).

TABLE 8. SELECTED INTERATOMIC DISTANCES (Å) AND ANGLES (°) FOR CATAMARCAITE

W	S1	S2	S2	S2
S1	**2.240(8)**	109.5(2)	109.5(2)	109.5(2)
S2	3.675(7)	**2.260(3)**	109.5(2)	109.4(2)
S2	3.675(7)	3.690(2)	**2.260(3)**	109.4(2)
S2	3.675(7)	3.690(4)	3.690(4)	**2.260(3)**
Cu1	**S4**	**S3**	**S2**	**S2**
S4	**2.274(4)**	114.4(2)	109.6(2)	109.6(2)
S3	3.843(9)	**2.299(5)**	109.2(1)	109.2(1)
S2	3.765(3)	3.775(6)	**2.333(3)**	104.5(2)
S2	3.765(3)	3.775(6)	3.690(2)	**2.333(3)**
Cu2	**S3**	**S3**	**S1**	**S2**
S3	**2.313(3)**	113.5(2)	108.5(2)	110.9(2)
S3	3.871(4)	**2.314(4)**	108.5(2)	110.9(2)
S1	3.764(3)	3.765(5)	**2.326(3)**	104.1(2)
S2	3.828(6)	3.829(6)	3.675(7)	**2.335(6)**
Ge	**S4**	**S3**	**S3**	**S3**
S4	**2.228(9)**	109.7(2)	109.7(2)	109.7(2)
S3	3.653(8)	**2.240(3)**	109.3(2)	109.3(2)
S3	3.653(9)	3.653(5)	**2.240(5)**	109.3(2)
S3	3.653(8)	3.653(4)	3.653(7)	**2.240(4)**

Sequence of Crystallization

Based on their textural relationships, the following sequence of crystallization is proposed for the Ge-bearing sulfides within bornite-rich ore at Capillitas: putzite → catamarcaite → unnamed $Cu_8Fe_2ZnGe_2S_{12}$ → briartite-type phase. Putzite is the oldest and the only Ag-bearing phase, and it usually occurs as anhedral relics in chalcocite (Paar *et al*. 2004b). Catamarcaite is rarely seen in direct contact with putzite (Fig. 3b), but it probably formed somewhat later. It is usually observed as anhedral to euhedral grains lining cavities and fractures in bornite – chalcocite – digenite matrix (Figs. 2, 3). Tungsten, a major element in catamarcaite, is derived from the decomposition of hübnerite (Fig. 2b). Putzite is commonly replaced by unnamed $Cu_8Fe_2ZnGe_2S_{12}$ (Paar *et al*. 2004b), and catamarcaite, by the briartite-type phase (Fig. 3c). These two minerals belong to the system Cu–Fe–Zn–Ge–S, and their deposition is probably related to secondary (supergene) processes of replacement.

Acknowledgements

WHP expresses his thanks to the Austrian Science Foundation (FWF) for supporting field and laboratory work in both Argentina and Austria (grant P 13974). HP gratefully acknowledges the hospitality of Miguel Yampa and his family (Andalgalá, Argentina) during the field seasons 2000, 2001 and 2002 at Capillitas. We thank Prof. Ricardo Sureda (University of Salta,

TABLE 9. POLYHEDRON CHARACTERISTICS FOR CATAMARCAITE

	1	2	3	4	5	6	7	8	9	10
W	4	2.255	0.0064	1	0	0.0192	1	48.031	5.884	5.76
Cu1	4	2.309	0.0185	1	0.0017	0.0545	1	51.541	6.304	1.19
Cu2	4	2.322	0.0067	1	0.0034	0.0199	1	52.421	6.401	1.15
Ge	4	2.237	0.0041	1	0	0.0124	1	46.889	5.745	3.82
S1	4	2.363	0.0519	1	0.4984	0.1478	1	55.285	3.398	2.35
S2	4	2.367	0.0452	1	0.5007	0.1295	1	55.562	3.399	2.26
S3	4	2.291	0.0226	1	0.0017	0.0664	1	50.384	6.162	1.84
S4	4	2.261	0.0147	1	0.0055	0.0436	1	48.419	5.9	1.96

Column headings: 1: coordination number, C.N., 2: sphere radius, 3: eccentricity, 4: sphericity, 5: epsilon, 6: volume eccentricity, 7: volume sphericity, 8: sphere volume, 9: polyhedron volume, 10: bond valence.

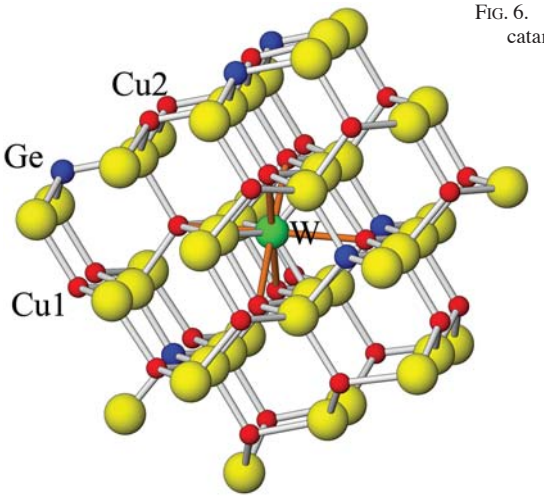

FIG. 6. Metal–metal contacts Cu–W in the crystal structure of catamarcaite. W is positioned in the inverted tetrahedron.

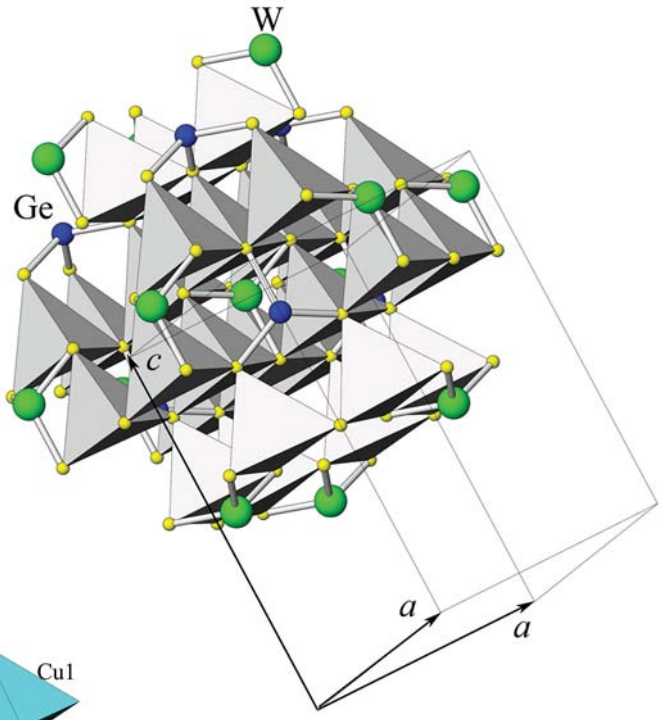

FIG. 7. A fragment of a double layer with cubic stacking and a W-containing inverted tetrahedron, bound by fragments of adjacent layers of tetrahedra, in a hexagonal stacking orientation; the lower one shows a vacancy in the tetrahedral site.

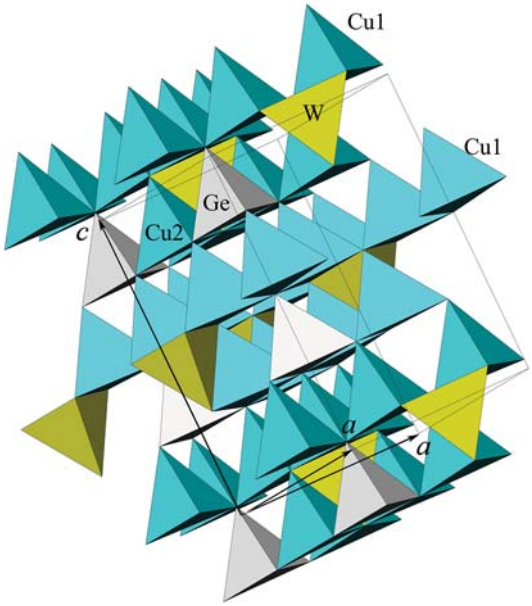

FIG. 8. Crystal structure of catamarcaite in a polyhedron representation. A stack of three consecutive double-layers (0001) are shown.

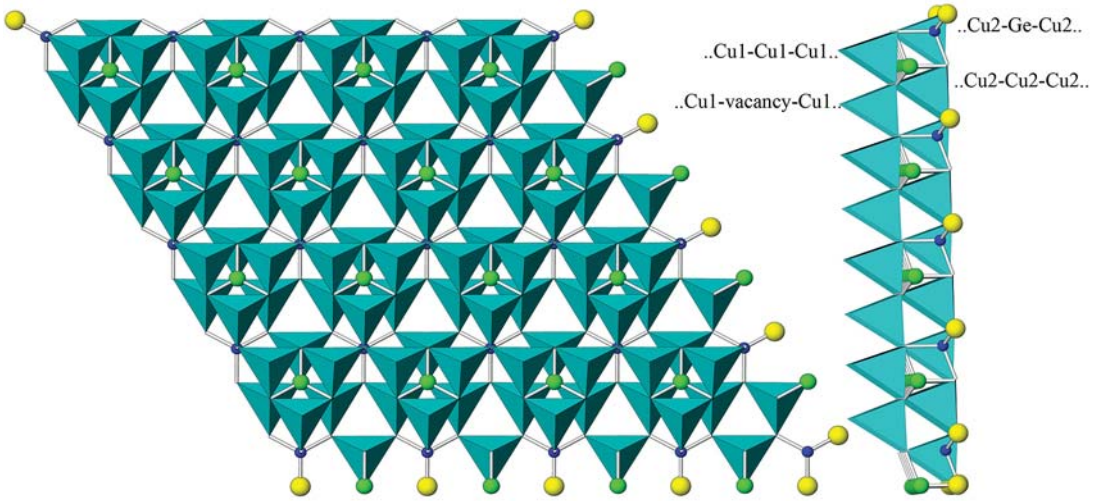

FIG. 9. A unit double-layer (with cubic stacking of component layers) from the crystal structure of catamarcaite. Blue tetrahedron: Cu1 and Cu2, small dark blue spheres: Ge, larger green spheres: W. Note the vacancies in the tetrahedral site in the upper component layer.

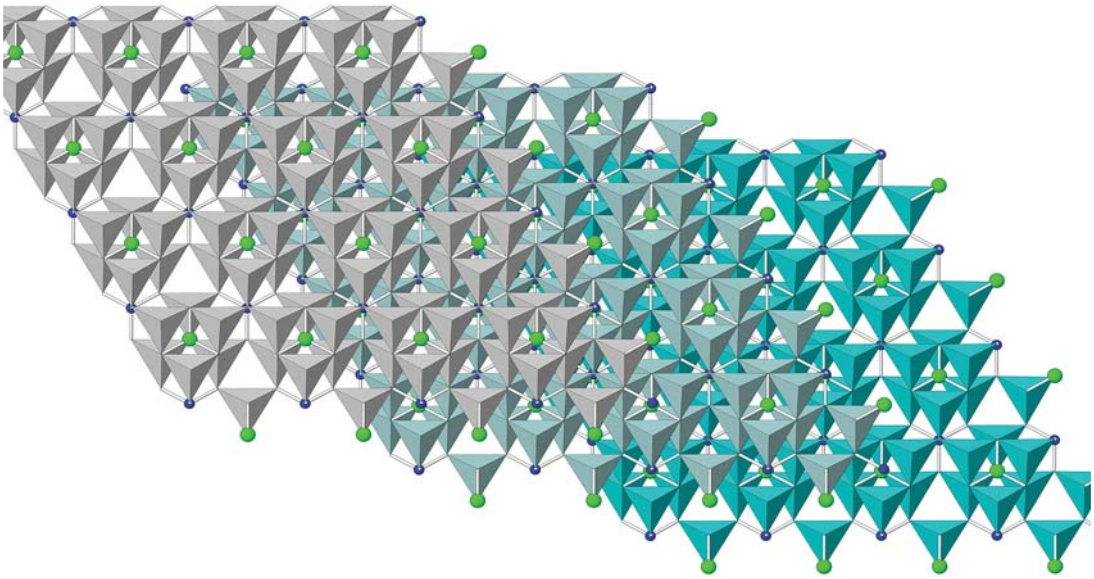

FIG. 10. A model of the crystal structure of kiddcreekite constructed by a sphalerite (cubic)-like stacking of double layers from Figure 9. Small blue spheres: Sn, large green spheres: W.

Argentina) for logistical help in Argentina, Georg Zagler (University of Salzburg) for the reflectance and microhardness measurements, and Winfried Waldhör (University of Salzburg) for the preparation of polished sections. The valuable comments of Robert F. Martin, Paul G. Spry, and two anonymous referees contributed to the improvement of this paper.

References

ACEÑOLAZA, F.G., TOSELLI, A.J., DURAND, F.R. & DÍAZ TADEI, R. (1982): Geología y estructura de la regíon norte de Andalgalá, Provincia de Catamarca. *Acta Geológica Lilloana* **16**, 121-139.

AHLFELD, F. & SCHNEIDER-SCHERBINA, A. (1964): Los yacimientos minerales y de hidrocarburos de Bolivia. *Departamento Nacional de Geología, La Paz, Bolivia, Boletin Especial* **5**.

ANGELELLI, V. & RAYCES, E. (1946): Estudio geológico-minero del distrito cuprífero Capillitas, Dpto. Andalgalá, Prov. Catamarca. Dirección General de Fabricaciones Militares, Buenos Aires, Argentina, unpubl. report.

BALIĆ-ŽUNIĆ, T. & VICKOVIĆ, I. (1996): IVTON: a program for the calculation of geometrical aspects of crystal structures and some crystal chemical applications. *J. Appl. Crystallogr.* **29**, 305-306.

BAUMANN, L., HOFMANN, F. & WEBER, W. (1997): *Glückauf Freiberg. Bergbau – Erze – Mineralien*. Bode Verlag, Haltern, Germany.

BERNSTEIN, L.R. (1985): Germanium geochemistry and mineralogy. *Geochim. Cosmochim. Acta* **49**, 2409-2422.

BREITENMOSER, T. (1999): *Geology and Geochemistry of the Calc-Alkaline Farallón Negro Volcanic Complex at Capillitas, NW-Argentina*. M.Sc. thesis, ETH Zürich, Switzerland.

BRUKER AXS (1998a): SMART, Version 5.0. Bruker AXS, Inc., Madison, Wisconsin 53719, U.S.A.

BRUKER AXS (1998b): SAINT+, Version 5.0. Bruker AXS, Inc., Madison, Wisconsin 53719, U.S.A.

BRUKER AXS (1998c): XPREP, Version 5.0. Bruker AXS, Inc., Madison, Wisconsin 53719, U.S.A.

CRIDDLE, A.J. & STANLEY, C.J. (1993): *The Quantitative Data File for Ore Minerals*. The Commission on Ore Mineralogy, International Mineralogical Association. Chapman & Hall, London, U.K.

FRANCOTTE, J., MOREAU, J. & OTTENBURGS, R. (1965): La briartite, $Cu_2(Fe,Zn)GeS_4$, une nouvelle espèce minérale. *Bull. Soc. fr. Minéral. Cristallogr.* **88**, 432-437.

GEIER, B.H. & OTTEMANN, J. (1970a): New primary vanadium-, germanium-, gallium-, and tin-minerals from the Pb–Zn–Cu-deposit Tsumeb, South West Africa. *Mineral. Deposita* **5**, 29-40.

GEIER, B.H. & OTTEMANN, J. (1970b): New secondary tin–germanium and primary tungsten- (molybdenum-, vanadium-) germanium minerals from the Tsumeb ore-deposit. *Neues Jahrb. Mineral., Abh.* **114**, 89-107.

GEIER, B.H. & OTTEMANN, J. (1972): Briartit, das dritte Germaniumsulfid-Mineral aus der Erzlagerstätte Tsumeb. *Neues Jahrb. Mineral., Abh.* **118**, 97-109.

HARRIS, D.C., ROBERTS, A.C., THORPE, R.I., CRIDDLE, A.J. & STANLEY, C.J. (1984): Kiddcreekite, a new mineral species from the Kidd Creek mine, Timmins, Ontario and from the Campbell orebody, Bisbee, Arizona. *Can. Mineral.* **22**, 227-232.

HUG, A. (1999): *Petrography and Genesis of the Capillitas Diatreme, Farallón Negro Volcanic Complex, NW-Argentina*. M.Sc. thesis, ETH Zürich, Switzerland.

INTIOMALE, M.M. & OOSTERBOSCH, R. (1974): Géologie et géochimie de gisement du Kipushi, Zaïre. *In* Gisements Stratiformes et Provinces Cuprifères (P. Bartholomé, ed.). Société Géologique de Belgique, Liège, Belgique (123-164).

KRAUS, W. & NOLZE, G. (1999): POWDERCELL 2.3. Federal Institute for Materials Research and Testing, Berlin, Germany.

LOMBAARD, A.F., GÜNZEL, A., INNES, J. & KRÜGER, T.L. (1986): The Tsumeb lead–copper–zinc–silver deposit, South West Africa/Namibia. *In* Mineral Deposits of Southern Africa (C.R. Anhaeusser & S. Maske, eds.). Geological Society of South Africa, Johannesburg, South Africa (1761-1787).

MÁRQUEZ-ZAVALÍA, M.F. (1988): *Mineralogía y genesis del yacimiento Capillitas* (*Catamarca, República Argentina*). Ph.D. thesis, University of Salta, Salta, Argentina.

MÁRQUEZ-ZAVALÍA, M.F. (1999): El yacimiento Capillitas, Catamarca. *In* Recursos Minerales de la República Argentina (O. Zappettini, ed.). *Instituto de Geología y Recursos Minerales SEGEMAR, Anales* **35**, 1643-1652.

PAAR, W.H. & PUTZ, H. (2005): Germanium associated with epithermal mineralization: examples from Bolivia and Argentina. *Eighth Biennial SGA Meeting* (*Beijing*), *Proc.* **3**, 48-51.

PAAR, W.H., PUTZ, H., TOPA, D. & ZAMBRANA MOGRO, J.M. (2004a): High grade silver–germanium mineralization at Porco, Department of Potosí, Bolivia. *32nd Int. Geol. Congress* (*Florence*), *Abstr.* (*part 2*), 1068.

PAAR, W.H., ROBERTS, A.C., BERLEPSCH, P., ARMBRUSTER, T., TOPA, D. & ZAGLER, G. (2004b): Putzite, $(Cu_{4.7}Ag_{3.3})_{\Sigma 8}GeS_6$, a new mineral species from Capillitas, Catamarca, Argentina: description and crystal structure. *Can. Mineral.* **42**, 1757-1769.

PUTZ, H. (2005): *Mineralogy and Genesis of Epithermal Ore Deposits at Capillitas, Catamarca Province, NW Argentina*. Ph.D. thesis, Salzburg Univ., Salzburg, Austria.

PUTZ, H., PAAR, W.H., SUREDA, R.J. & ROBERTS, A.C. (2002): Germanium mineralization at Capillitas, Catamarca Province, Argentina. *Int. Mineral. Assoc., 18th Gen. Meeting* (*Edinburgh*), *Abstr.*, 265.

SASSO, A.M. (1997): *Geological Evolution and Metallogenetic Relationships of the Farallón Negro Volcanic Complex, NW Argentina*. Ph.D. thesis, Queen's Univ., Kingston, Ontario.

SASSO, A.M. & CLARK, A.H. (1998): The Farallón Negro group, northwest Argentina: magmatic, hydrothermal and tectonic evolution and implications for Cu–Au metallogeny in the Andean back-arc. *Soc. Econ. Geol., Newsletter* **34**, 1-18.

SCLAR, C.B. & GEIER, B.H. (1957): The paragenetic relationships of germanite and renierite from Tsumeb, South West Africa. *Econ. Geol.* **52**, 612-631.

SHANNON, R.D. (1976): Revised effective ionic radii and systematic studies of interatomic distances in halides and chalcogenides. *Acta Crystallogr.* **A32**, 751-767.

SHELDRICK, G.M. (1997a): SHELXS–97. A Computer Program for Crystal Structure Determination. University of Göttingen, Göttingen, Germany.

SHELDRICK, G.M. (1997b): SHELXL–97. A Computer Program for Crystal Structure Refinement. University of Göttingen, Göttingen, Germany.

SHIMIZU, M., STANLEY, C.J., CRIDDLE, A.J., KATO, A. & MATSUBARA, S. (1991): New compositional and optical data for antimonian and bismuthian varieties of hemusite from Japan. *Mineral. Petrol.* **45**, 11-17.

SILLITOE, R.H. & HEDENQUIST, J.W. (2003): Linkages between volcanotectonic settings, ore-fluid compositions, and epithermal precious metal deposits. *Soc. Econ. Geol., Spec. Publ.* **10**, 315-343.

SPIRIDONOV, E.M. (1994): New germanium–molybdenum–tungsten sulfide mineral phases from the massive sulfide-polymetallic Tsumeb deposit (Namibia). *Geol. Ore Deposits* **36**, 335-341.

SPIRIDONOV, E.M. (2003): Maikanite $Cu_{20}(Fe,Cu)_6Mo_2Ge_6S_{32}$ and ovamboite $Cu_{20}(Fe,Cu,Zn)_6W_2Ge_6S_{32}$: new minerals in massive sulfide base metal ores. *Dokl. Acad. Sci. USSR, Earth Sci. Sect.* **393A**, 1329-1332.

SPIRIDONOV, E.M., KACHALOVSKAYA, V.M., KOVACHEV, V.V. & KRAPIVA, L.YA. (1992): Germanocolusite $Cu_{26}V_2(Ge,As)_6S_{32}$: a new mineral. *Vestnik Moskovskogo Universiteta, Seriya 4, Geologiya* **1992**(6), 50-54 (in Russ.).

TERZIEV, G.I. (1971): Hemusite – a complex copper–tin–molybdenum sulfide from the Chelopech ore district, Bulgaria. *Am. Mineral.* **56**, 1847-1854.

VIAENE, W. & MOREAU, J. (1968): Contribution à l'étude de la germanite, de la renierite et de la briartite. *Ann. Soc. Géol. Belg.* **91**, 127-143.

WAGNER, T. & MONECKE, T. (2005): Germanium-bearing colusite from the Waterloo volcanic-rock-hosted massive sulfide deposit, Australia: crystal chemistry and formation of colusite-group minerals. *Can. Mineral.* **43**, 655-669.

YAMANAKA, T. & KATO, A. (1976): Mössbauer effect study of ^{57}Fe and ^{119}Sn in stannite, stannoidite and mawsonite. *Am. Mineral.* **61**, 260-265.

YOUNG, B.B. & MILLMAN, A.P. (1964): Microhardness and deformation characteristics of ore minerals. *Inst. Mining Metall. Trans.* **73**, 437-466.

Received November 4, 2005, revised manuscript accepted May 26, 2006.